Effect of Two-Dimensional Conduction Heat Transfer on Thermal Margin of Reactor Vessel Lower Head

Chan-Soo Kim, Kune Y. Suh

Seoul National University

San 56-1 Shinrim-dong, Kwanak-gu, Seoul, 151-742, Korea

Abstract

As an in-vessel retention design concept, external cooling of the reactor vessel has been suggested to protect the lower head from overheating due to relocated material from the core. The effectiveness of the ex-vessel management may be estimated by the thermal margin defined as the ratio of the critical heat flux to the actual heat flux from the outer surface of the reactor vessel. Principal factors affecting the thermal margin calculation are the amount of heat to be transferred downward from the molten pool, variation of heat flux with angular position, two-dimensional conduction in the vessel wall, and finally the amount of removable heat by external cooling. The results are presented for the thermal margin as the thickness of the vessel wall varies from 0.05m to 0.15m and 0.25m. The results are also presented for the thermal margin accounting for the existence of the cylinder part of the reactor beltline which contributes to conducting the heat upward.

1. Introduction

Recently, the COrium Attack Syndrome Immunization Structures (COASIS) are being developed as prospective in-vessel retention devices for a next-generation water reactor at the Seoul National University. Both the engineered gap cooling structures in-vessel (COASISI) and ex-vessel (COASISO) were demonstrated to maintain effective heat transfer geometry during molten core debris attack when applied to the TMI-2 and the Korean Standard Nuclear Plant (KSNP) reactors.

Boiling has long been recognized as one of the most efficient ways of cooling hot or heated surfaces, which is of fundamental importance in many applications in nuclear and chemical industries. However, most of boiling research was focused on upward facing geometry and performed in the experiments using small objects. Thus there is a scarcity of data with direct applicability to cooling the hemispherical reactor lower head externally on a major scale. Recently, a limited number of studies did examine the external cooling of nuclear reactor vessel downward facing hemispherical surface.

El-Genk and Gao [1] studied pool boiling of water from downward-facing hemisphere. In this paper, quenching experiments were conducted to investigate pool boiling of saturated water on downward-facing aluminum and 303E stainless steel hemispheres.

Theofanous and Syri [2] performed several external cooling experiments at the ULPU experimental facility. Their experiments are divided into configurations I, II, and III. Configuration I experiment established the lower limits of coolability under lower submergence, pool boiling conditions. Using configuration II experiments, they considered the heat flux shape, full submergence and natural circulation in the reactor lower head.

Rouge [3] performed the SULTAN experiment to study large-scale structure coolability by water in boiling natural convection. The objective was to measure the main characteristics of two-dimensional, two-phase flow so as to evaluate the recirculation mass flow in the large system. His result suggested that the heat flux exceeding 1MW /m^2 may be removed under natural water circulation conditions, provided that the water circuit is well designed and optimized.

Park & Jeong [4] presented the thermal margin for external reactor vessel cooling in a large advanced light water reactor (ALWR). They chose Steinberner & Reineke' s [5] Nusselt number for upward natural convection and Theofanous et al.' s [6] Nusselt number and Mayinger et al.' s [7] Nusselt number for downward convection, respectively. They also cited the correlation based on the Mini-ACOPO [6] experimental data in order to find the angular heat flux distribution and calculated the critical heat flux (CHF) at the outer surface of the lower head using Theofanous and Syri [2] correlation developed from the ULPU-2000 configuration II experiment.

Nomenclature

A	surface area of the control volume [m^2]	h_{nc}	nucleate boling heat transfer coefficient [W/m^{2}K]
c_p	specific heat [J/kgK]		
F	correction factor for Cheung' s CHF	H	water level [m]
g	gravitational acceleration [m/s^2]	H'	pool depth [m]
h_{fg}	latent heat of vaporization [J/kg]	Ja	Jakob number

k	thermal conductivity [W/mK]	q	angular coordinate; azimuthal angle
L	local liquid head [m]	r_g	saturated vapor density [kg/m^3]
L_b	length ratio between the intrinsic bubble size and the vessel radius	r_f	saturated liquid density [kg/m^3]
		s	surface tension [N/m]
Nu	Nusselt number	**Subscripts**	
p	pressure [N/m^2]	CHF	critical heat flux
Q_v	volumetric heat rate [W/m^3]	i,j	index of a temperature node
q''	heat flux [W/m^2]	M	outer surface
r	radial coordinate	p	pool
Ra'	modified Rayleigh Number	sat	saturated state
T	temperature [K]	V	volumetric
z	z-coordinate	**Superscripts**	
a	thermal diffusivity [m^2/s]	D	lower surface of control volume
b	volumetric expansion coefficient [K^{-1}]	L	left surface of control volume
Δ	finite increment	R	right surface of control volume
u	kinematic viscosity [m^2/s]	U	upper surface of control volume

2. Model Description

In this chapter we mainly explain the factors affecting the thermal margin calculations. The factors influencing thermal margin calculations are the amount of heat to be transferred downward in the pool, the azimuthal variation of the local heat flux, the local heat flux on the outer surface of the vessel and finally the maximum removable heat to the coolant submerging the vessel lower head. The first two factors account for the natural convection and the last factors are two-dimensional conduction heat transfer and external cooling. The geometric and thermal boundary conditions shown in Figure 1 were used to calculate the local heat flux on the outer surface. To evaluate the thermal margin, we resort on the information on the heat removal capacity suggested by Theofanous and Syri [2] and Cheung et al. [8].

2.1 Themal Load

To estimate the thermal margin, we need the heat input to the vessel from the internal pool. The amount of heat source explained in this section is determined from the decay heat that is dependent on shutdown time, the amount of heat transferred to the downward surface by the natural convection for the total decay power and the azimuthal variation of the decay heat. In this study, we assumed that the decay heat is 0.7% of total operating power of 4000MWt. The

reason we chose the value of 0.7% is to obtain the thermal margin after the debris has accumulated and solidified in the reactor vessel lower head.

To investigate the amount of heat transferred downwards by the natural convection, we chose five reference cases listed in Table 1.

Despite a great deal of studies performed so far, there exist yet no applicable data readily applicable to reactor conditions. Further, most of the tests were performed with relatively low Rayleigh number as compared to a postulated severe accident condition (above 1.0×10^{17}). In the literature, the modified Rayleigh number, Ra', is defined as follows:

$$Ra' = \frac{gbQ_vH'}{k_p a_p v_p} \qquad (1)$$

To cover a wide spectrum of the thermal margin, we chose the data having different geometries (i.e. rectangular, semicircular, hemispherical and torispherical geometries) of which some of the data were based on the experiment, while other data were based on the numerical study. The respective references suggested different Nusselt numbers for different directions so that the fraction of the heat transferred downwards varied with the used correlation. Figure 2 shows the values of heat split fraction for the different correlations surveyed in this study.

For all the experimental studies carried out so far, we assumed that the heat flux from the debris bed in the reactor vessel lower head to the outside wall varies azimuthally. For years, a number of investigators have studied the heat flux from the debris to the reactor vessel lower head. They concentrated on several natural convection experiments in the lower head vessel.

In this study, we need the correlation of the experimental data for the heat transfer coefficient varying with the local position. Several investigators proposed correlations based on the experimental data, some of which are compared in Figure 3. Jahn & Reineke's [9] experimental data, Suh & Henry's [10] correlation and the new correlation by Yoon [11] are typically shown in Figure 4.

2.2 Local heat flux on the outer surface of the vessel

To obtain the local heat flux on the outer surface of the vessel, we solved two-dimensional steady-state conduction equations in spherical and cylindrical coordinates. The boundary condition for the inner surface was the azimuthal variation of the local heat flux on the inner surface. The boundary condition for the outer wall was the nucleate boiling on the outer surface of the vessel as given by h=20,000 W/m²K. The finite difference method was used to solve the differential equations as:

$$0 = k_{i,j}^L A_{i,j}^L \frac{T_{i,j-1} - T_{i,j}}{r_i \Delta q} + k_{i,j}^R A_{i,j}^R \frac{T_{i,j+1} - T_{i,j}}{r_i \Delta q} + k_{i,j}^U A_{i,j}^U \frac{T_{i-1,j} - T_{i,j}}{\Delta r} + k_{i,j}^D A_{i,j}^D \frac{T_{i+1,j} - T_{i,j}}{\Delta r} \qquad (2)$$

$$0 = k_{i,j}^L A_{i,j}^L \frac{T_{i,j-1} - T_{i,j}}{\Delta z} + k_{i,j}^R A_{i,j}^R \frac{T_{i,j+1} - T_{i,j}}{\Delta z} + k_{i,j}^U A_{i,j}^U \frac{T_{i-1,j} - T_{i,j}}{\Delta r} + k_{i,j}^D A_{i,j}^D \frac{T_{i+1,j} - T_{i,j}}{\Delta r} \tag{3}$$

Equation (2) is the two-dimensional conduction equation in the spherical coordinates, while equation (3) is that in the cylindrical coordinates.

The thermal conductivity of carbon steel was taken from Stickler et al. [12]. The thicknesses of the vessel wall was varied from 0.05 to 0.15 and 0.25 m. We examined the cases with and without the cylindrical portion of the vessel. The error of this analysis was within ± 0.0001 °C. The local heat flux was determined as follows:

$$q_j'' = h\left(T_{M,j} - T_{sat}\right) \tag{4}$$

2.3 Heat removal capacity

The last factor to calculate the thermal margin is the heat removal capacity by external cooling. Generally this capacity is represented by the CHF, which is the value for the maximum heat removal by water. In this study, two references were chosen. One is the result of Theofanous and Syri's correlation [2] developed from the ULPU-2000 configuration II experiment:

$$q_{CHF}'' = 490 + 30.2\boldsymbol{q} - 8.88 \times 10^{-1}\boldsymbol{q}^2 + 1.35 \times 10^{-2}\boldsymbol{q}^3 - 6.65 \times 10^{-3}\boldsymbol{q}^4 \; kW/m^2 \tag{5}$$

As the experimental apparatus of the ULPU-2000 configuration II was set up as the closed loop, the above equation yielded the CHF value for the case of the forced convective boiling. The other one is Cheung et al.'s result [8]. They intended to establish a proper scaling law, developed a design correlation for prediction of the CHF on the exterior surface of a real-size reactor vessel. Their correlation takes the following form:

$$q_{CHF}'' = F_{L_b} F_P F_{\boldsymbol{q}} F_{Ja} \tag{6}$$

The correlation consists of the four functions. The function F_{L_b} is a size correction factor. In view of the fact that the local buoyancy force that is parallel to the curved heating surface is proportional to $g\sin\boldsymbol{q}$, the effect of vessel size is expected to vary with the local angular position, $\boldsymbol{q}$. Thus the size correction factor, F_{L_b} is dependent on both L_B and $\boldsymbol{q}$. Using a power-law expression, the equation of F_{L_b} is as follows:

$$F_{L_b}(L_b, \boldsymbol{q}) = \exp\!\left[0.8 L_b^{0.5}(\sin\boldsymbol{q})^{0.333}\right], \qquad L_B = \frac{1}{R}\left[\frac{\boldsymbol{s}}{g(\boldsymbol{r}_l - \boldsymbol{r}_g)}\right]^{0.5} \tag{7}$$

Even though L_B varies by four orders of magnitude due to the relatively larger radius of the vessel than that of the intrinsic bubble size, the spatial variation function varies within ± 5%. A least-square fits gives

$$F_{\boldsymbol{q}}(\boldsymbol{q}) = 0.0473\left(1 + 1.78\boldsymbol{q} - 0.51\boldsymbol{q}^2\right) \tag{8}$$

where $\boldsymbol{q}$ is in radians.

The function F_P is the property or pressure function given by

$$F_P(P) = \rho_g h_{fg} \left[\frac{\sigma g(\rho_l - \rho_g)}{\rho_g^2} \right]^{0.25} \left(1 + \frac{\rho_g}{\rho_l} \right)^{0.33}$$

(9)

The value F_P depends on the fluid properties varying with the system pressure.

For pool boiling, the effect of subcooling can be represented as a linear function of the Jakob number, Ja, as

$$F_{Ja}(Ja) = 1 + 19.25 \, Ja, \quad Ja = \frac{c_p \Delta T_{sub}}{h_{fg}}$$

(10)

The water level, H, is measured from the external bottom center of the vessel. The local liquid head, L at a given angular position on the hemispherical heating surface is given by

$$L = H - R(1 - \cos\theta)$$

(11)

It follows that the difference between the local water pressure at θ and the system pressure above the water surface is

$$\Delta P = \rho_l g H \left(1 - \frac{R}{H} \cos\theta \right) \quad \text{for } 0 \leq \theta \leq \frac{\pi}{2}$$

(12)

The local liquid head from equation (12) maintains the water on the hemispherical heating surface subcooled. Thus, if the saturation temperature at the free surface is 100°C, the subcooled condition due to that local liquid head is as follows:

$$\Delta T_{sub} = 2.54 H \left[1 - \frac{R}{H} (1 - \cos\theta) \right] \left\{ 1 - 0.0192 H \left[1 - \frac{R}{H} (1 - \cos) \right] \right\}$$

(13)

From equations (10) and (13), the function F_{Ja} for the subcooling is given by

$$F_{Ja} = 1 + 0.0914 H \left[1 - \frac{R}{H} (1 - \cos\theta) \right] \left\{ 1 - 0.0192 H \left[1 - \frac{R}{H} (1 - \cos\theta) \right] \right\}$$

(14)

In this study, the water level H is 7.017 m, the length from the external bottom center of the vessel to the top of the active fuel of the Korean Next Generation Reactor (KNGR) and the radius of the lower head is 2.5362m. Figure 5 shows the critical heat flux at all angular positions utilizing Theofanous and Syri' s [2] and Cheung et al.' s [8] models.

3. Discussion of Results

We chose Mayinger et al' s [7] correlation which yields the largest fraction of the downward heat transfer in five correlations for the natural convection.

3.1 Critical heat flux

Figure 5 shows that Theofanous and Syri' s [2] critical heat flux values at all angular positions are always larger than those of Cheung et al.' s [8] not considering the local liquid head. Figure 5 also shows that the critical heat flux values at all angular positions of Theofanous and Syri [2]

are always lower than those of Cheung et al. [8] considering the local liquid head except at the top. It results from the subcooled effect due to local liquid head. Because of the decrease of subcooled effect at the top, Theofanous and Syri's [2] CHF values are higher than those of Cheung et al.'s [8] at the top. We chose Cheung et al.'s CHF [8] considering the local liquid head. Figure 6 also shows that the CHFR from the three CHF at the same condition share the same trend.

3.2 Effect of cylinder part

Figure 7 shows that the cylinder part has varying degrees of influence on the local heat flux with the angular positions when thickness is 0.25m. The cylinder part has little influence on the local heat flux at the bottom. But it tends to decrease the local heat flux on the outer wall at the top. Figure 8 also shows the same effect for the CHFR.

3.3 Effect of thickness

Figure 9 shows the local heat flux with the angular positions in three cases of thickness. Figures 10 and 11 show that the local heat flux is the highest in 0.25m thickness at the top, but that the local heat flux is the highest in 0.05m thickness at the bottom. Thus, the CHFR at the top where CHFR is the lowest value was higher than suggested by Yoon [11] by conduction heat transfer as illustrated in Figure 12. Figure 13 carries the following message that for the thickness 0.05m the difference is observed to be minimal between the local heat flux with the cylinder part and that without the cylinder part. For the thickness of 0.25m the difference is amplified between the local heat flux with the cylinder part and that without the cylinder part. Thus, the thicker vessel, the greater the influence of the cylinder part. Figure 14 also shows the same effect for the CHFR in the top region.

4. Conclusion

According to this study, it is certain that the top region of the lower head vessel of the reactor is thermally more susceptible to failure (i.e. melting), while the heat removal capacity at the top is larger than that at the bottom. This is mainly due to the natural convection phenomenon in the molten pool. But thermal margin is increased by two-dimensional conduction heat transfer at the top. Especially, at the top the CHFR increase diminishes the potential for the vessel failure by the metal layer. In the real case the forced convection effect, static and dynamic pressure addition due to the small flow area at the top may increase the CHFR.

References

1. El-Genk M.S. and Gao C., 1999, "Experiments on Pool Boiling of Water from Downward-facing Hemisphere," *Nuclear Technology*, vol. 125, pp.52-69

2. Theofanous T. G. and Syri S., 1997, "The coolability limits of a reactor vessel lower head," *Nuclear Engineering and Design,* vol. 169, pp.59-76

3. Rouge S., 1997, "SULTAN test facility for large scale vessel coolability in natural convection at low pressure," *Nuclear Engineering and Design*, vol. 169, pp. 185-195

4. Park J. W. and Jeong D. W., 1997, "An investigation of thermal margin for external reactor vessel cooling (ERVC) in large advanced light water reactor (ALWR)," Proceedings of the Korean Nuclear Society Spring Meeting, Kwangju, Korea, vol.1, pp. 473-478

5. Steinberner U. and Reineke H. H., 1978, "Turbulent buoyancy convection heat transfer with internal heat sources," Proceeding of the Sixth International Heat Transfer Conference, Toronto, Canada, August

6. Theofanous T. G. et al, 1995, "In-vessel coolability and retention of a core melt*," DOE/ID-10460*, vol. 1, U.S. Department of Energy, Washington, DC, USA.

7. Mayinger F., Jahn M, Reineke H.H. and Steinberner U., 1975, "Examination of thermohydraulic process and heat transfer in a core melt," Final report BMFT RS 48/1, Technical University of Hannover, Germany

8. Cheung F. B., Haddad K. H. and Liu Y. C., 1997, "Critical heat flux phenomenon on a downward facing curved surface," *NUREG/ CR- 6507 PSU/ME-97-7321*

9. Jahn M. and Reineke H. H., 1974, "Free convection heat transfer with internal heat sources," Proceedings of the Fifth International Heat Transfer Conference, vol. 3, Tokyo, Japan

10. Suh K. Y. and Henry R. E., 1994, "Integral analysis of debris material and heat transport in reactor vessel," *Nuclear Engineering and Design*, vol. 151, pp. 203-221

11. Yoon H.J, 1999, "Two-phase heat removal from the downward facing hemispherical

geometry," M.S. Thesis, Department of Nuclear Engineering, Seoul National University, Seoul, Korea

12. Stickler L.A. et al., 1994, "Calculations to estimate the margin to failure in the TMI-2 vessel," *NUREG/CR-6196 TMI V(93)EG01 EGG-2733*

13. Kelkar K. M. and Patankar S. V., 1993, "Computational modeling of turbulent natural convection in flows simulating reactor core melt," Innovative Research Inc., Final Report submitted to Sandia National Laboratories, Albuquerque, NM, USA.

14. Kymäläinen O., Tuomisto H., and Thefanous T. G., 1993, "Heat flux distribution from a volumetrically heated pool with high Rayleigh number," Proceedings of the Sixth Nuclear Reactor Thermal Hydraulics, Grenoble, France

15. Asfia F. J. and Dhir V. K., 1994, "An experimental study of natural convection in a volumetrically heated spherical pool with rigid wall," International Mechanical Engineering Congress & the Winter Annual Meeting, Chicago, IL, USA., November 6-11

16. Park H. J., Dhir V. K. and Kastenberg W. E., 1994, "Effect of external cooling on the thermal behavior of a boiling water reactor vessel lower head," *Nuclear Technology*, vol. 108, pp. 266-282

17. Mayinger F., Fritz M.,Reineke H.H., Rinkleff L., Schramm R., and Steinberner U., 1980, "Theoretical and Experimental Research on the Behavior of a Core Melt on Reactor Containment and on the Basement Concrete," FB(RS-166-79-05), Germany

Table 1 Summary of natural convection correlation

Geometry	Correlation	Ra'	Pr	Reference Type of Data
Rectangular	$Nu_{up} = 0.345 Ra'^{0.253}$ $Nu_{side} = 0.85 Ra'^{0.19}$ $Nu_{down} = 1.389 Ra'^{0.0095}$	1×10^7 ~ 1×10^{11}	7	Steinberner & Reineke [5] Experimental
Semicircular	$Nu_{up} = 0.4 Ra'^{0.2}$ $Nu_{down} = 0.55 Ra'^{0.2}$	7×10^6 ~ 5×10^{14}	7	Mayinger et al. [17] Numerical
Hemispherical	$Nu_{up} = 0.345 Ra'^{0.233}$ $Nu_{down} = 0.0038 Ra'^{0.23}$	1×10^{12} ~ 1×10^{15}	2.5 ~ 11	Theofanous et al. [6] Experimental
Hemispherical	$Nu_{up} = 0.18 Ra'^{0.237}$ $Nu_{down} = 0.1 Ra'^{0.25}$	1×10^6 ~ 1×10^{16}	1	Kelkar & Patankar [13] Numerical
Torispherical	$Nu_{up} = 0.345 Ra'^{0.233}$ $Nu_{side} = 0.85 Ra'^{0.19}$ $Nu_{down} = 0.54 Ra'^{0.18}(H/R)^{0.26}$	1×10^{13} ~ 1×10^{15}	7	Kymäläinen et al. [14] Expermental
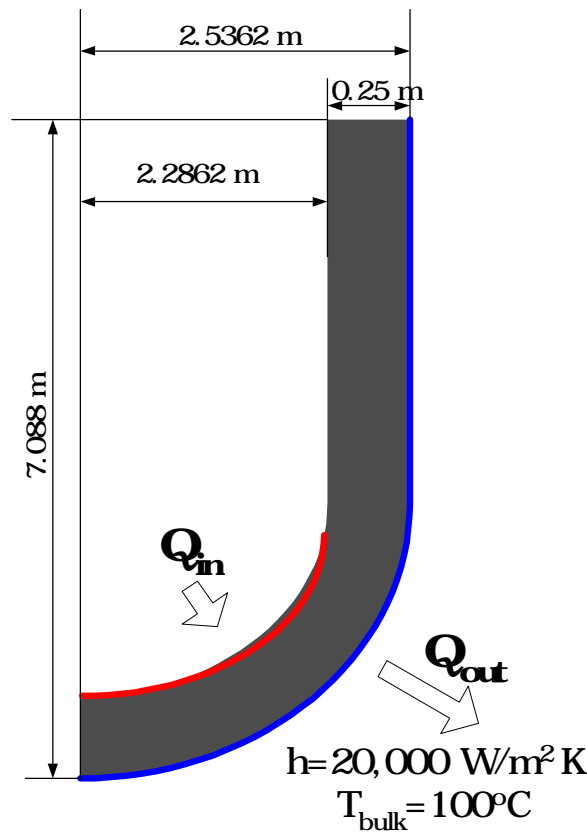
Figure 1 Geometric and thermal boundary conditions for this analysis
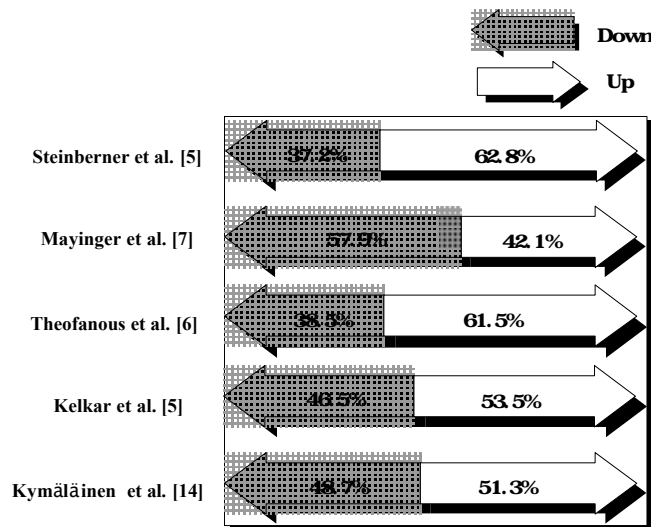
Figure 2 Heat split factors for different natural convection correlations
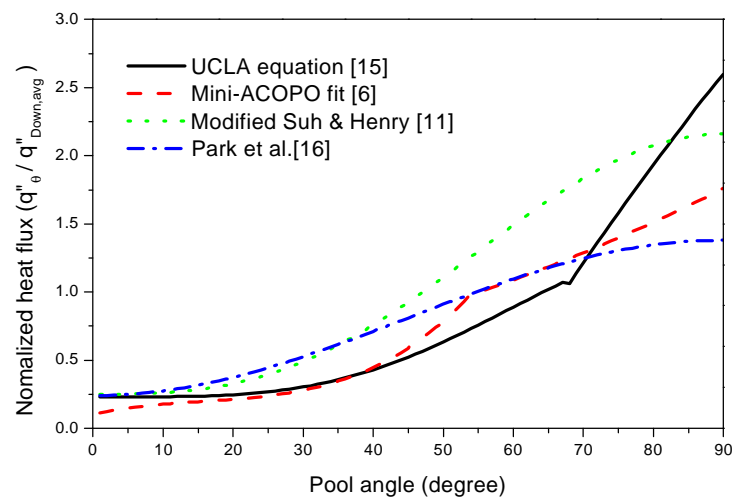
Figure 3 Azimuthal variation of heat flux from the natural convection
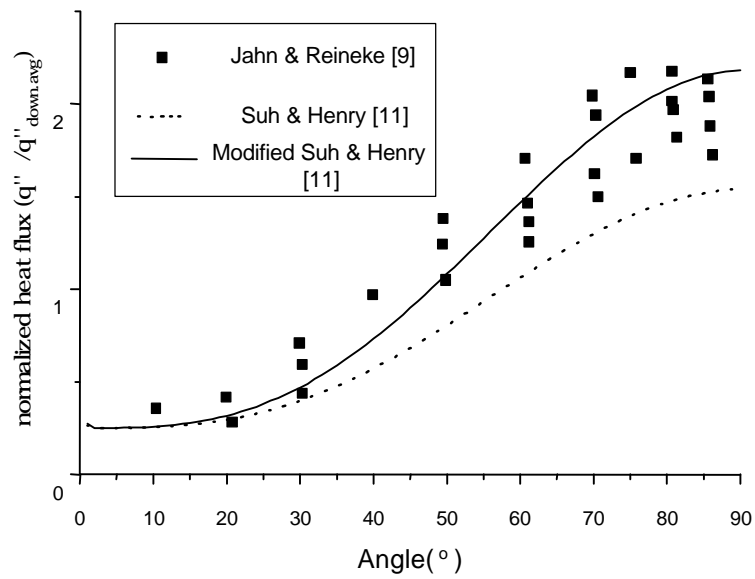
Figure 4 New fitting correlation for the data of John & Reineke
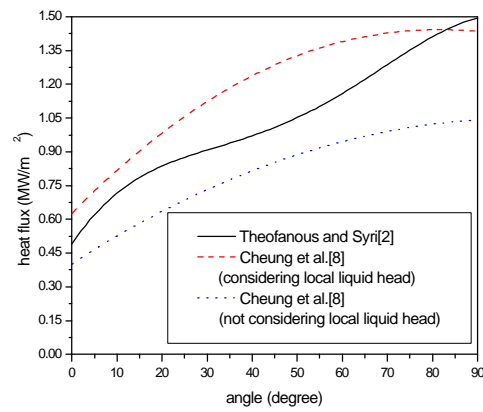
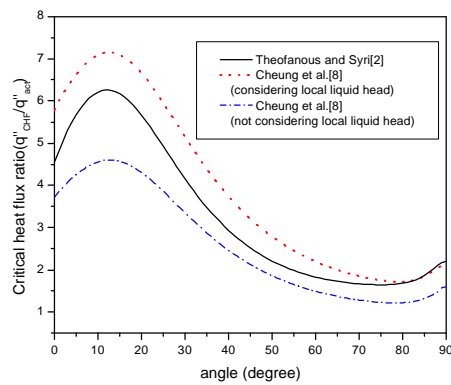Figure 5 Critical heat flux in pool boiling
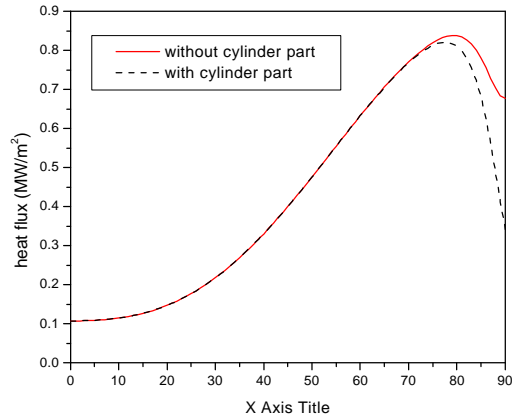

Figure 6 CHFR from three CHF values

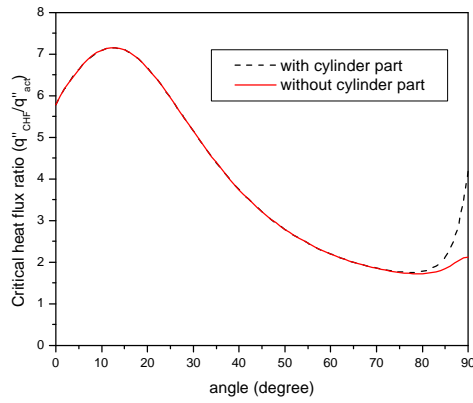Figure 7 The local heat flux on the outer surface with the cylinder part induced or not

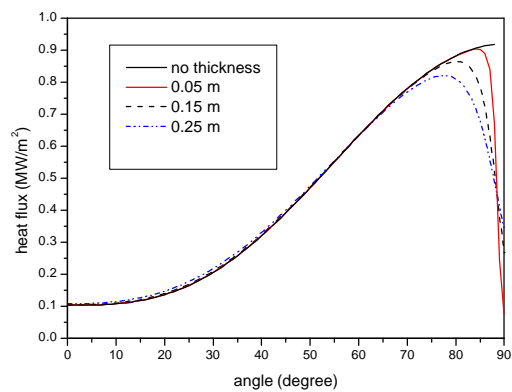Figure 8 CHFR with the cylinder part induced or not

Figure 9 The local heat flux on the outer surface

at all angular positions as a function of thickness
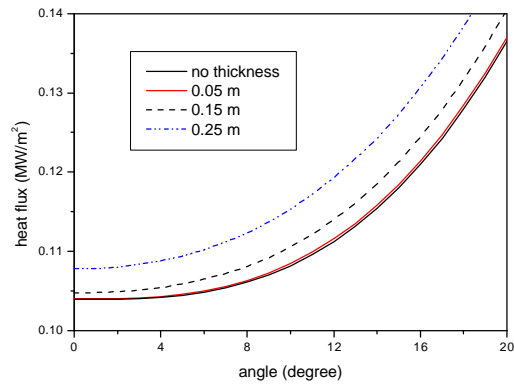
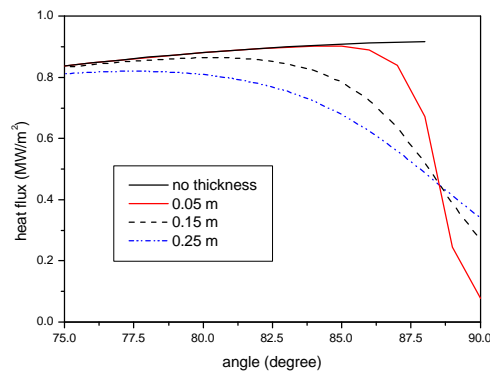Figure 10 The local heat flux on the outer surface
at the bottom region as a function thickness

Figure 11 The local heat flux on the outer surface
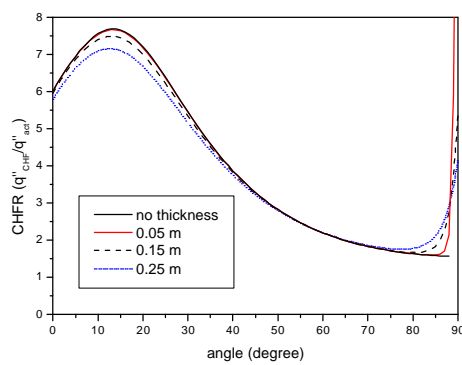at the top region as a function thickness
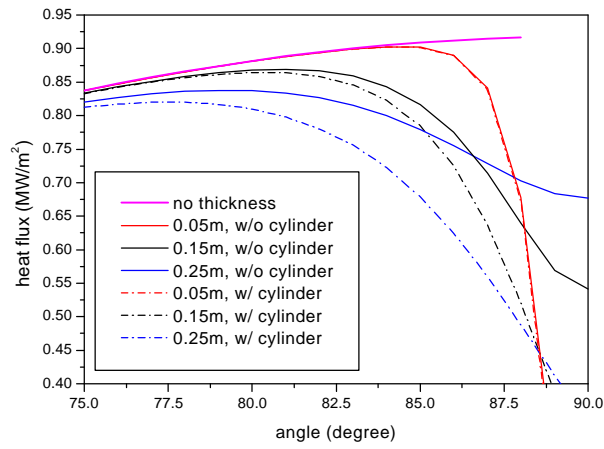

Figure 12 Thermal margins as function of thickness

Figure 13 The local heat flux on the outer surface for all the case in this work
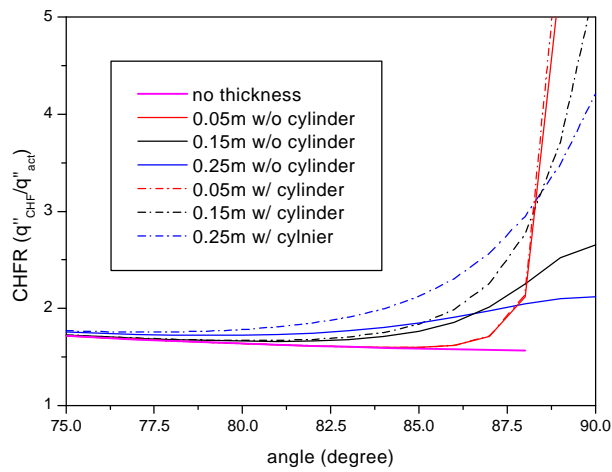

Figure 14 CHFR on the outer surface for all the case in this work